

## ZNO-Ag/PS and ZnO/PS Films for Photocatalytic Degradation of Methylene Blue

Hassan Khuder Naji<sup>1</sup>, Amjed Mirza Oda<sup>1,\*</sup>, Wesam Abduljleel<sup>2</sup>,  
Hussein Abdilkadhim<sup>2</sup>, and Rawaa Hefdhi<sup>2</sup>

<sup>1</sup>Science Department, College of Basic Education, University of Babylon, Babylon 51002, Iraq

<sup>2</sup>Department of Chemistry, College of Sciences, University of Babylon, Babylon 51002, Iraq

\* **Corresponding author:**

tel: +964-7812475243

email: almajid1981@yahoo.com

Received: November 27, 2018

Accepted: March 27, 2019

DOI: 10.22146/ijc.41347

**Abstract:** Two films of ZnO-Ag/polystyrene (ZnO-Ag/PS) and ZnO/polystyrene (ZnO/PS) have been prepared and the photodegradation ability of stabilized catalysts was evaluated for methylene blue (MB) degradation. The efficiency of ZnO improved against recombination of electron-hole pair by modification of catalyst surface with Ag photodeposition to be more resistant towards photocorrosion. ZnO-Ag catalyst was characterized by SEM and EDS analysis to show high roughness of this catalyst and Ag deposited on the surface was 2% (molar ratio). ZnO-Ag/PS and ZnO/PS composites were made as films and were then analyzed by FTIR spectra that showed the interaction of ZnO and ZnO-Ag with polystyrene appeared in the range of 400–620  $\text{cm}^{-1}$ , XRD pattern indicated the presence of Ag nanoparticles on the surface of ZnO and ZnO/PS film has maximum absorbance at 376 nm in UV-VIS spectra. This value shifted to 380 nm because of the photodeposition. The photocatalytic reaction was depicted using MB in the UV-irradiation action of stacked films in MB solution. The result showed that both ZnO-Ag/PS and ZnO/PS films gave efficiency to remove MB by 97% and 70%, respectively. The reusability test of the films showed that ZnO-Ag/PS was more resistant than ZnO/PS. The presence of Ag also increased the efficiency in photodegradation and resistance against photocorrosion.

**Keywords:** photocatalysis; photodeposition; ZnO-Ag; methylene blue

### ■ INTRODUCTION

Photocatalysis techniques are new eco-friendly methods for environmental treatments to decontaminate dyes in the wastewater. Metal oxide semiconductors as heterogeneous photocatalyst are an important material that utilized by many applications in industry and many technological processes like environmental and biomedical applications [1-2]. One of the serious problems in wastewater is contamination with an organic and inorganic dye that discharged to aquatic habit, which will add high risk to living organisms leading to pollution crises. Dyes are powerful coloring agent in the textile and leather industry.

On the other hand, these dyes are non-biodegradable when expelled to the ecosystem and resisted degradation so that it will cause health problems

according to carcinogenic nature. Also, their presence made problem in an aquatic system like low illumination reaching the bottom and low oxygen demand [3-4]. Dyes can be removed using photocatalysis reaction in the presence of titanium dioxide ( $\text{TiO}_2$ ) and zinc oxide (ZnO), and these catalysts can harvest light energy for photodegradation and significantly enhance the rate of degradation [5].

Semiconductor catalyst such as ZnO, when illuminated with photons forms in the valence band (VB) a positive hole ( $\text{h}^+$ ) and the conduction band (CB) an electron ( $\text{e}^-$ ). The positive hole oxidized by hydroxyl ions to produce hydroxyl radicals ( $\text{OH}^*$ ) and causing degradation of organic contaminants directly or indirectly. In the conduction band, the electron is consumed by adsorbed oxygen and forms oxygen superoxide. These species enhance the rate of

degradation by destroying the chemical structure through several steps of oxidation, reaching mineralization the dyes converting into CO<sub>2</sub> and H<sub>2</sub>O [6-7].

TiO<sub>2</sub> is most widely used in photocatalysis to decontamination of dyes, but ZnO also has similar activity to be useful like TiO<sub>2</sub> where its band gap energy is 3.2 eV. ZnO has a relatively lower cost of production and ease in the separation of electrons and holes charges. Thus ZnO can be used as an alternative catalyst instead of TiO<sub>2</sub> [8-10]. However, the capability of ZnO in photodegradation opposite its poor chemical stability under photocatalytic reaction [11] as it undergoes corrosion by self-oxidation under UV irradiation, leading to the loss of the photocatalytic activity. Thus, it needs to improve the photostability by incorporation into various composites like TiO<sub>2</sub> or by deposition of noble metals like Ag on the surface [5,12].

Efficient photocatalytic degradation of organic pollutants was reported by depositing TiO<sub>2</sub> ultrathin layer on Ag-ZnO nanorods, where the addition of Ag work as a sink for electron collector and prevent charges recombination. The TiO<sub>2</sub> layer increases the stability of photocatalyst against photo-corrosion under UV irradiation [12]. Several studies have designated that the photocatalytic rate increases with catalyst loading with metal, but at high concentrations of metal load will lose its efficiency, because of light scattering and screening effects happened [13]. Also, photodegradation is more efficient in case of increasing the lifetime of electron-hole separation and retarding recombination. According to this method, incorporation of species that accept electrons at conduction band of the photocatalyst, like transition metal ions or oxides increases the activity in degradation comparing to bare semiconductors. The consuming of a photo-excited hole by photooxidation species are expected could reduce the recombination process and make it highly efficient [5,12,14]. Usually, defect in photocatalyst by doping makes shifting in band gap to less value; therefore, the addition of dopants decrease the band gap causing surface modification by the new site and lifetime charges carriers' recombination is retarded and increase the photocatalyst ability in the photodegradation process [15-16].

In many previous reports, the photocatalytic reaction usually constructed according to the common protocol, where the photocatalyst is used as a powder and added to the dye solution with stirring to get a slurry, then illuminated with proper source of light to initiate the photocatalytic reaction. This protocol is limited to be used in industrial treatment units, because the recovery of catalyst and takes more times for continuing the treatment units work or expelled the catalyst to the environment, leading another problem. In our previous study, the photocatalyst is stabilized on a surface like cotton fiber by impregnation of in ZnO and ZnO-Ag and used for photodegradation of safranin O dye [17-18]. In addition, silver incorporation in TiO<sub>2</sub> and a polystyrene matrix was made to remove dye from wastewater as a floating photocatalyst [19]. Zinc oxide nanoparticles were also fixed on glass plates as a photocatalyst to remove Acid Red 88 dye in aqueous solution [20]. This strategic way reported that mixing the photocatalyst with polymer matrix gives a new technique in water purification with characteristic features like good photocatalytic activity, low cost in consuming of the catalyst and no need to recover the catalyst after water treatment [21].

Thus in this study, the action of ZnO doped Ag and comparison of photodegradation of methylene blue solution were demonstrated, where MB is likely used as an example to evaluate the photodegradation efficiency [22]. In the presence of ZnO/PS and ZnO-Ag/PS, both of them are stabilized in the polystyrene matrix controlling the photocatalyst to be not expelled to the environment. Some analysis like UV Vis, FTIR, XRD, SEM, EDS spectroscopy was used. The photodegradation of dye solution against time and the reusability of the films were also monitored and studied.

## ■ EXPERIMENTAL SECTION

### Materials

Zinc oxide (ZnO) and methylene blue dye was supplied by Fluka Co., silver nitrate from BDH, polystyrene from local markets, acetone and chloroform by GCC, and were used without further purification.

## Instrumentation

UV VIS spectra were recorded for polystyrene, ZnO/PS and ZnO-Ag/PS films in the range 200-800 nm using UV VIS spectrophotometer LF 4030, Scienco (Korea) by cutting pieces of the films ( $2 \times 1$ ) cm and inserted in the UV VIS holder to record the spectra and blank holder was air. FTIR analysis is done directly for the films and tested using Affinity IR instrument (Shimadzu, Japan) recorded in the range  $400\text{--}4000\text{ cm}^{-1}$ , where the films located directly in the FTIR holder to record the spectra. XRD diffraction of ZnO and ZnO-Ag are characterized by XRD apparatus (DX-2700 SSC, USA) using the films in the range  $20\text{--}60^\circ$  of the diffraction angle ( $2\theta$ ). ZnO-Ag was analyzed by Scanning Electron Microscope Inspect 550, Netherland. EDS of ZnO-Ag was tested using energy dispersion X-ray (EDX), Bruker Nano GmbH, Germany, where the powder is suspended in absolute ethanol, and the suspension dropped on a piece of aluminium for SEM and EDS analysis.

## Procedure

### **Preparation of composite of ZnO-Ag by photodeposition**

ZnO powder about 5 g was weighed and suspended in 100 mL of a mixture of distilled water/Acetone (50:50) with stirring for 1 h. Silver nitrate was then added to the suspension, where the ratio of Ag was 2.5% molar ratio related to ZnO weight. The suspension was radiated using ultraviolet lamps (Phillips, 70 W) for 4 h, where this time all silver ion completely deposited on ZnO surface.  $\text{AgNO}_3$  was added to the filtrate of ZnO suspension to ensure no  $\text{AgCl}$  precipitate is formed. Finally, the white suspension turned into grey color and continuing until the maximum of the solvent is evaporating. ZnO-Ag composite was then filtrated and washed with distilled water several times and dried at  $80^\circ\text{C}$  for 12 h. This sample is prepared for analysis like SEM and EDS.

### **Preparation of ZnO-Ag/PS and ZnO/PS film**

Polystyrene (0.95 g) was dissolved in 20 mL of chloroform using magnetic stirrer for 3 h in reflux apparatus and followed by the addition of 0.05 g of ZnO or ZnO-Ag with continuous stirring for 30 min to get a

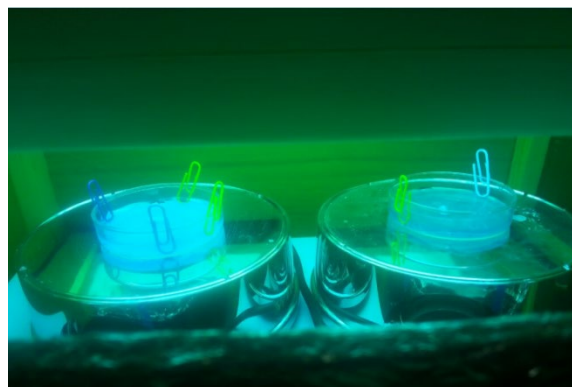


**Fig 1.** Photocatalytic degradation reaction installation (Petri dishes contain ZnO/PS film on the left and ZnO-Ag/PS film on the right were immersed in 10 ppm of methylene blue solution)

thick dispersed solution. After a slurry was formed, it was then poured in Petri dishes and left to evaporate in room temperature for 24 h to get casted films of ZnO/PS and ZnO-Ag/PS. The film without catalysts, which is polystyrene only, was used as a control film. These films are directly characterized by XRD, FTIR, and UV VIS spectroscopy.

### **Photocatalytic degradation reaction**

Photocatalytic degradation ability of ZnO-Ag and ZnO films was evaluated by the degradation of methylene blue under 70 watt UV lamp. In the degradation procedure, the film of ZnO-Ag/PS, ZnO/PS, or PS were stacked in 5 cm diameter Petri dish reaching the base of the dish with metal buckle, keeping the film against floating and most of the solution will be above the film as shown in Fig. 1. Then 10 mL of methylene blue solution (10 ppm) was added with ensuring most of the solution is above the film; it was then stirred for 15 min in the dark until the adsorption/desorption equilibrium was reached. This is enough time for adsorption according to the amount of catalyst in the PS matrix, that is only 5% w/w. The UV lamp was applied about 10 cm above the Petri dish, and the maximum absorbance of methylene blue was measured at 665 nm using UV-vis spectrophotometer scan between 200–800 nm wavelengths recorded every 15 min.

## ■ RESULTS AND DISCUSSION

ZnO-Ag/PS, ZnO/PS, and PS films were characterized by FTIR analysis and appeared in Fig. 2. The common main peaks are the same with no shifting, except after catalyst mixing leads to strong absorption at 400–550  $\text{cm}^{-1}$ . Absorption bands at 3100  $\text{cm}^{-1}$  belong to aromatic C-H stretching. The values of 2920  $\text{cm}^{-1}$  and 2850  $\text{cm}^{-1}$  absorption are assigned to  $\text{CH}_2$  group for the asymmetric and symmetric stretching vibrations respectively. Aromatic C=C stretching peaks appeared at 1600 and 1500  $\text{cm}^{-1}$ . The C-H deformation vibration band of benzene ring hydrogen appeared at 950  $\text{cm}^{-1}$ . Also, the mono-substituted ring showed absorption peaks at 759 and 654, while the main peak of ZnO in the ZnO/PS composite was observed at the range 400–550  $\text{cm}^{-1}$ . When compared to this value with recent works of literature, it is similar to this work [23-24].

UV-Vis spectrum of PS, ZnO/PS, and ZnO-Ag/PS are shown in Fig. 3, the PS does not show any appreciable absorption, and there is only a broad and less intense

absorption band in the Vis region, while its absorption is 200–250 nm. For the composite films, it can be seen that there is UV absorption in all the samples, in the range of 240–390 nm, where the presence of zinc oxide enhances the UV absorption capacity of PS film. The ZnO content enhances the UV shielding properties of the polymer. When the number of dopant atoms increased, the gap of a semiconductor is lowered. Ag acts as a dopant that work as photo-sensitizer, which induce the separation of electron-hole pairs and prevent their recombination. Thus, the dopant works as a bridge to transfer charges between the localized states [25]. Moreover, slight redshifts from 376 to 380 nm for the absorption peaks are observed in ZnO-Ag/PS film as a result of Ag doping. Such redshifts of the edge of absorption peaks of ZnO have also been reported [26].

XRD analysis was performed to analyze the degree of crystallinity and nature of ZnO and ZnO-Ag composites, with  $\text{CuK}\alpha$  radiation (40 Kv, 30 mA). The diffraction of X-ray showed spectra of ZnO/PS and

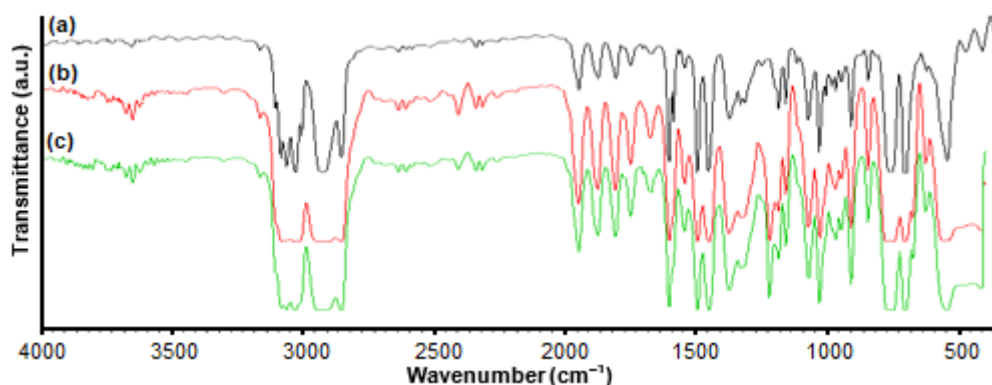


Fig 2. The FTIR spectra of (a) polystyrene films, (b) ZnO/PS films, and (c) ZnO-Ag/PS films

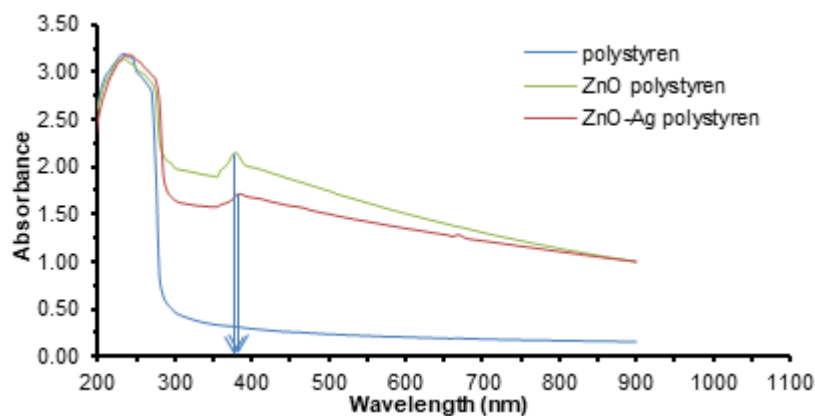


Fig 3. UV VIS spectra of PS, ZnO/PS, and ZnO-Ag/PS

ZnO-Ag/PS composites. Characteristic peaks appeared in the range of  $2\theta$  values of  $20\text{--}60^\circ$ , where the presence of several peaks indicating that the crystallinity of the composite is high, as shown in Fig. 4.

According to Fig. 4, ZnO-Ag peaks indicating the presence of silver and ZnO phases and no other structure is formed after doping. This means ZnO and Ag metal are the only phases that are found after photodeposition with successive reduction of Ag ion on to ZnO surface. XRD data for all studied samples are observed that the essential peaks occur at Miller indexes (100), (002), (101), (102), and (110), where the diffraction peaks are  $31.80$ ,  $34.41$ ,  $36.21$ ,  $47.52$ , and  $56.53$ . The main peaks of ZnO are similar to the ZnO phase liked wurtzite (hexagonal) structure, according to JCPDS card no. 36-1451. The new peak at  $38.05^\circ$  in ZnO-Ag/PS spectra does not belong to ZnO, but it is an indication of the presence of a silver particle in the (111) crystal plane that rapped on ZnO

surface. As the amount of Ag is low, the x-ray will not be sensitive to all diffracted peaks like  $44.38$  angle, thus (200) crystal planes of silver would not appear in the spectra [27].

ZnO-Ag composite was analyzed by SEM instrument to show the morphology of this photocatalyst and showed highly roughness, and the particles are distributed as dimensional form, which gives a good feature in surface area. Fig. 5(a) shows the SEM image of ZnO-Ag composite, and Fig. 5(b) is the EDS analysis of ZnO-Ag, and according to this test, the composite contained Zn, O, and Ag only. The presence of Ag peak indicates the successful modification of ZnO by Ag using photodeposition method. EDS analysis showed the atomic percentage that the amount of silver deposit on ZnO was 2%, while the percentage of Ag in the solution to prepare ZnO-Ag was 2.5% and this is a good result, where the error was low.

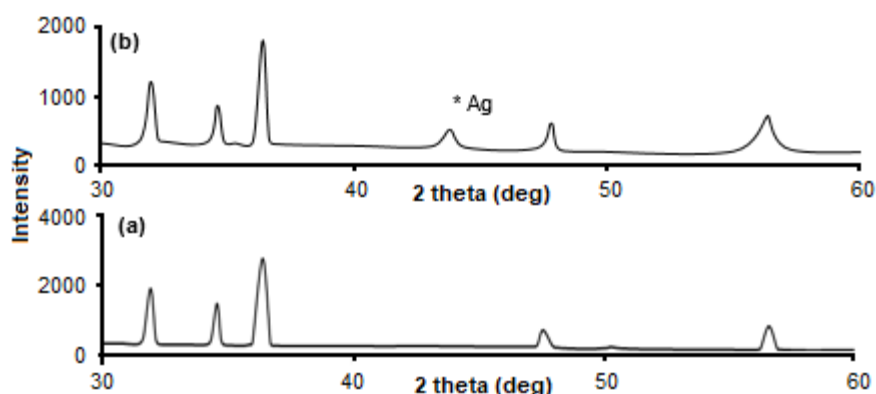


Fig 4. XRD of (a) ZnO/PS and (b) ZnO-Ag/PS

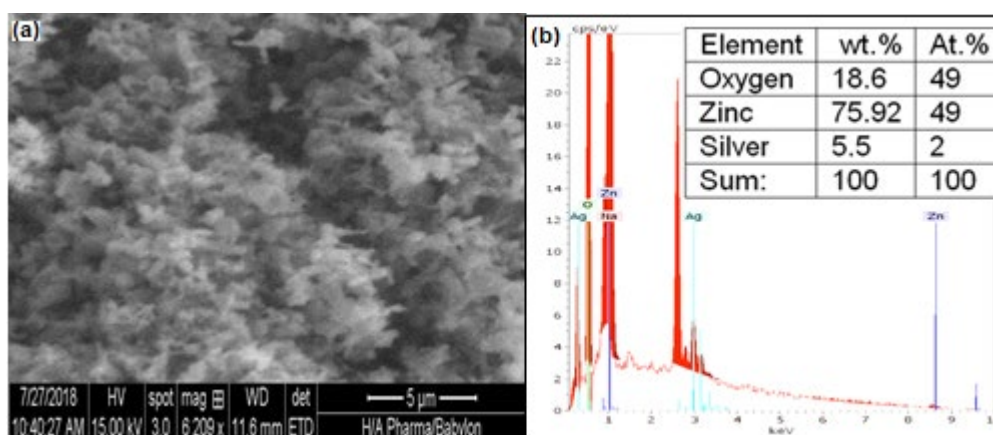


Fig 5. (a) SEM image and (b) EDS analysis of ZnO-Ag (the inserted table is weight and atomic elements percentage of ZnO-Ag)



Photocatalytic degradation activity of ZnO/PS and ZnO-Ag/PS were studied by degrading of MB dye under UV-irradiation in comparison to PS film. MB dye has maximum absorption at 665 nm, and the absorption is monitored to evaluate the photodegradation of MB, where in case of PS film there is a slight change in MB absorption, and this indicates the PS film has poor photocatalytic degradation.

In the case of ZnO-Ag/PS and ZnO/PS films, MB absorption is decreased with time due to the vanishing color by photocatalytic reaction, and this decreasing is continuing until the color of MB is disappeared. Fig. 6 shows the UV VIS spectra of MB solution with a concentration of 10 ppm in the presence of UV irradiation with proceeding time. In Fig. 6(a), the photodegradation of MB is very low as there is no photocatalyst, where PS film without catalyst, and the MB absorption was slightly changed related to initial concentration. Fig. 6(b) represents the effect of MB photodegradation by ZnO/PS film, and it can be seen that

the absorption of MB is changing in time proceeding. This also revealed that MB degraded by the action of ZnO/PS film is a good method to eliminate the dyes from industrial textile effluent. The degradation of MB solution using ZnO-Ag/PS catalyst is shown in Fig. 6(c); MB was more degradable in the same conditions in comparison with ZnO-Ag/PS and PS films. According to this result, the degradation activity will be more efficient as much as exposing to UV irradiation. Finally, the color tends to be colorless of MB as the full destruction of chemical structure.

PS as a polymer has low degradation activity and this regards to wide bandgap; therefore, it did not show any degradation of MB solution. ZnO-Ag/PS was more effective in MB removal than ZnO/PS film, and this attributed to the Ag doping. This modification changed the surface nature and made new active sites, increasing the surface area. Also, the photocatalytic activity of ZnO-Ag/PS was enhanced due to metallic Ag deposition on the surface of ZnO, and this metal works as electrons

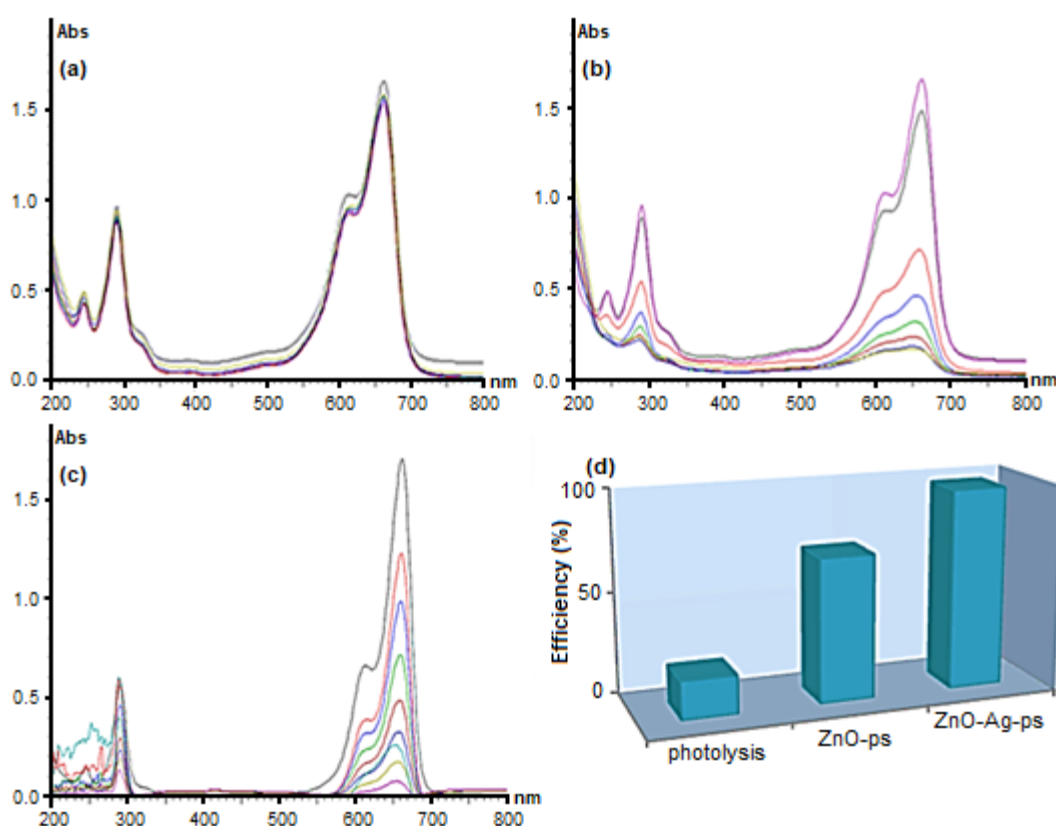


**Fig 6.** Photodegradation of MB by (a) PS film, (b) ZnO/PS film, (c) ZnO-Ag/PS film, and (d) efficiency of photodegradation of the three films

collectors. Silver nanoparticles that trapped on ZnO surface modify the surface with new geometrical active sites. This modification leads to change the electronic properties and increase the separation time of the electron-hole pair to give more time for electron trapping. Electrons trapped tend to move to an oxidized agent like the adsorbed molecular oxygen, and this prevents the recombination of electron-hole pairs. Thus the degradation efficiency was increased [28-29].

In addition, the ZnO-Ag/PS ability in MB degradation result from the electron-hole could have more than one pathway for the formation of electron-hole with more time and forbidding recombination as the three different interfaces of ZnO-Ag composite. The comparison of the photodegradation efficiency of the three films is shown in Fig. 6(d), where high efficiency of ZnO-Ag/ps film in the same conditions is reached up to 97% for 120 min after reaction, while ZnO/ps was 70% and PS film alone was 19% and this result is similar as reported [30].

The photocatalytic reaction of films against MB removal kinetics was studied, and it found that this kind of reaction follows pseudo-first-order kinetics. The most mechanism that follow this reaction is a Langmuir-Hinshelwood mechanism. This mechanism can explain

the degradation activity of heterogeneous photocatalyst. Depending on the concentration of MB dye, when the concentration of MB dye is low, the rate expression can be written as  $d[C]/dt = k[C]$ .  $k$  is the apparent constant of first-order rate calculated by the linear regression of the equation  $k = \ln(C_{MB0}/C_{MB})/t$ , where  $C_{MB0}$  and  $C_{MB}$  are the concentrations of MB dyes at the irradiation time 0 and  $t$  min, respectively. Plots of  $\ln(C/C_0)$  against the time of irradiation gives a straight line, as shown in Fig. 7, and the slope of the linear fitted line represents the value of  $k$ . The calculated  $k$  values were equal to 0.0284, 0.0253, and 0.0007  $\text{min}^{-1}$  for ZnO-Ag/PS, ZnO/PS, and PS films, respectively. It is obvious that ZnO-Ag/PS has a high degradation rate of MB dye under UV irradiation. According to these results, ZnO-Ag/PS can be used as treatment techniques to eliminate pollution by dyes through effluent wastewater [31-33].

The efficiency of MB photodegradation is clearly obvious in the presence of the photocatalyst ZnO/PS and ZnO-Ag/PS and PS. However, the amount of catalysts in the matrix in polystyrene film is low. ZnO/PS and ZnO-Ag/PS were highly active to diminish the color of MB, where ZnO-Ag/PS was very efficient as a result of a combination of Ag on ZnO surface. Fig. 8 shows the efficiency of photodegradation by UV light only, and the

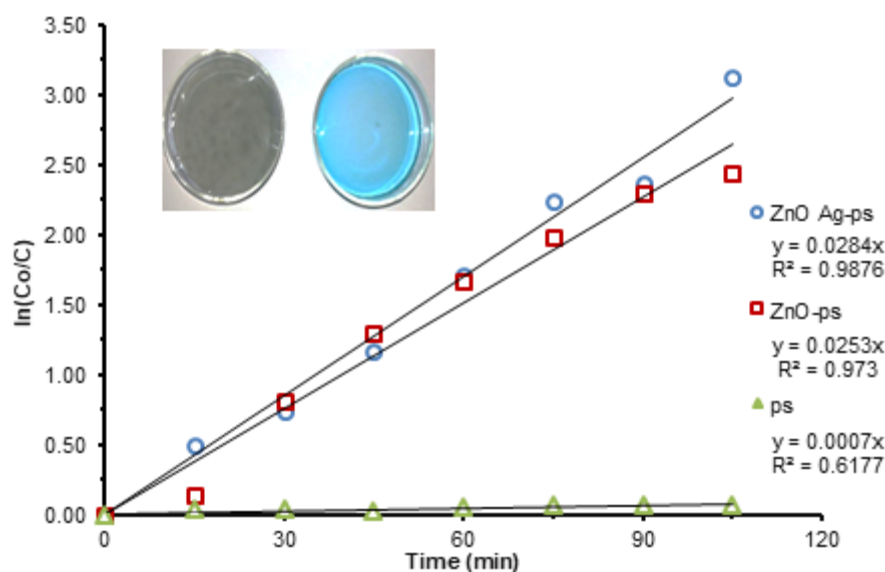


**Fig 7.** The first order plot of MB photodegradation (a) PS film, (b) ZnO/Ag film, (c) ZnO-Ag/PS film. The insight picture is Petri dishes of MB solution without catalyst on the right and with ZnO-Ag/PS film on the left at the end of the reaction

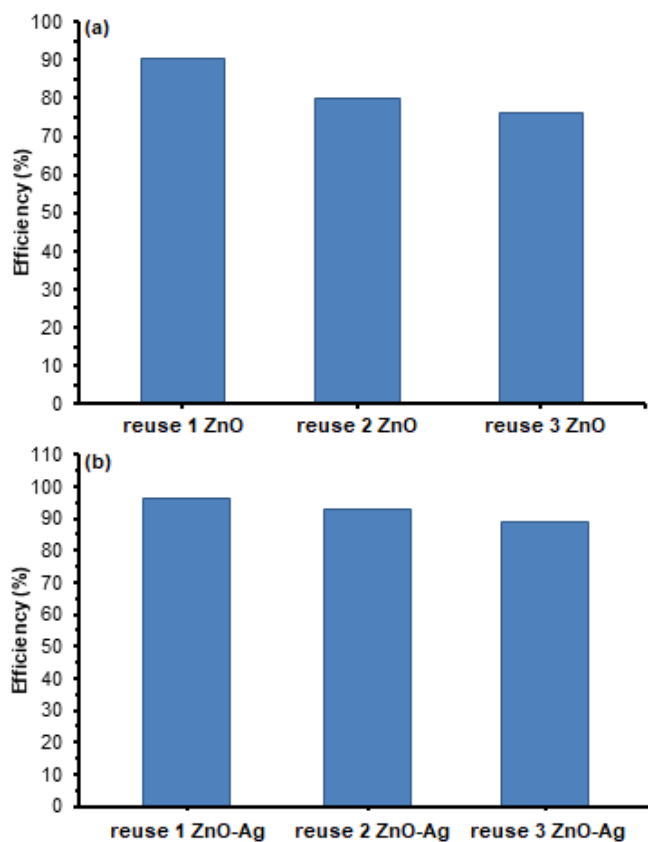


**Fig 8.** Photodegradation efficiency after reusing the (a) ZnO/PS and (b) ZnO-Ag/PS films

catalyst of ZnO/PS and ZnO-Ag/PS efficiency, which was 20, 80, and 96%, respectively. Another aspect of this study was testing the photodegradation activity after several runs, reusing the film again to ensure that the films can be used several times and measuring their efficiency in the degradation of MB. This experiment was accomplished by decanting the solution of MB after decolorization and replaced by a new solution of MB and illuminated by UV light, and the absorbance was measured so that the efficiency is calculated. Fig. 8 shows the efficiency of ZnO/PS and ZnO-Ag/PS films after were used in the first photodegradation and reused three times. ZnO/PS and ZnO-Ag/PA films have good reusability of photodegradation efficiency. The reusability of the catalysts is a benefit for cost-effectiveness to reduce the consumption of catalyst films each photodegradation process as reported [34-35].

## ■ CONCLUSION

ZnO and ZnO-Ag stabilized in polystyrene matrix give high efficiency in photocatalytic degradation of MB and had good reusability. Photodeposition of Ag on ZnO surface made a surface modification, according to the analysis of XRD, SEM, and EDS, making the MB degradation using ZnO-Ag/PS film was higher than using ZnO/PS film. In the same period of MB degradation, ZnO-Ag/PS efficiency was 97%, while it was 70% for ZnO/PS film. ZnO-Ag/PS film can be reused three times with the efficiency reached 89% compared to ZnO/PS film, which was 76%.

## ■ REFERENCES

- [1] Sangpour, P., Hashemi, F., and Moshfegh, A.Z., 2010, Photoenhanced degradation of methylene blue on cosputtered M:TiO<sub>2</sub> (M = Au, Ag, Cu) nanocomposite systems: A comparative study, *J. Phys. Chem. C*, 114 (33), 13955–13961.
- [2] Li, D., Zhang, Y., Wu, W., and Pan, C., 2014, Preparation of a ZnO/TiO<sub>2</sub> vertical-nanoneedle-on-film heterojunction and its photocatalytic properties, *RSC Adv.*, 4 (35), 18186–18192.
- [3] Teh, C.M., and Mohamed, A.R., 2011, Roles of titanium dioxide and ion-doped titanium dioxide on photocatalytic degradation of organic pollutants (phenolic compounds and dyes) in aqueous solutions: A review, *J. Alloys Compd.*, 509 (5), 1648–1660.
- [4] Josephine, G.S., and Sivasamy, A., 2014, Nanocrystalline ZnO doped on lanthanide oxide Dy<sub>2</sub>O<sub>3</sub>: A novel and UV light active photocatalyst for environmental remediation, *Environ. Sci. Technol. Lett.*, 1 (2), 172–178.
- [5] Zhao, H., Deng, W., and Li, Y., 2018, Atomic layer deposited TiO<sub>2</sub> ultrathin layer on Ag-ZnO nanorods for stable and efficient photocatalytic degradation of RhB, *Adv. Compos. Hybrid Mater.*, 1 (2), 404–413.
- [6] Ahmed, S., Rasul, M.G., Martens, W.N., Brown, R., and Hashib, M.A., 2010, Heterogeneous



- photocatalytic degradation of phenols in wastewater: A review on current status and developments, *Desalination*, 261 (1-2), 3–18.
- [7] Zheng, Y., Chen, C., Zhan, Y., Lin, X., Zheng, Q., Wei, K., and Zhu, J., 2008, Photocatalytic activity of Ag/ZnO heterostructure nanocatalyst: Correlation between structure and property, *J. Phys. Chem. C*, 112 (29), 10773–10777.
- [8] Sapkota, A., Anceno, A.J., Baruah, S., Shipin, O.V., and Dutta, J., 2011, Zinc oxide nanorod mediated visible light photoinactivation of model microbes in water, *Nanotechnology*, 22 (21), 215703.
- [9] Khodja, A.A., Sehili, T., Pilichowski, J.F., and Boule, P., 2001, Photocatalytic degradation of 2-phenylphenol on TiO<sub>2</sub> and ZnO in aqueous suspensions, *J. Photochem. Photobiol., A*, 141 (2-3), 231–239.
- [10] Chakrabarti, S., Chaudhuri, B., Bhattacharjee, S., Das, P., and Dutta, B.K., 2008, Degradation mechanism and kinetic model for photocatalytic oxidation of PVC–ZnO composite film in presence of a sensitizing dye and UV radiation, *J. Hazard. Mater.*, 154 (1-3), 230–236.
- [11] Sridharan, K., Jang, E., Park, Y.M., and Park, T.J., 2015, Superior photostability and photocatalytic activity of ZnO nanoparticles coated with ultrathin TiO<sub>2</sub> layers through atomic-layer deposition, *Chem. Eur. J.*, 21 (52), 19136–19141.
- [12] Fan, Y., Han, D., Song, Z., Sun, Z., Dong, X., and Niu, L., 2017, Regulations of silver halide nanostructure and composites on photocatalysis, *Adv. Compos. Hybrid Mater.*, 1 (2), 269–299.
- [13] Pareek, V.K., and Adesina, A.A., 2004, Light intensity distribution in a photocatalytic reactor using finite volume, *AIChE J.*, 50 (6), 1273–1288.
- [14] Pouretedal, H.R., Norozi, A., Keshavarz, M.H., and Semnani, A., 2009, Nanoparticles of zinc sulfide doped with manganese, nickel and copper as nanophotocatalyst in the degradation of organic dyes, *J. Hazard. Mater.*, 162 (2-3), 674–681.
- [15] Rauf, M.A., Meetani, M.A., Khaleel, A., and Ahmed, A., 2010, Photocatalytic degradation of methylene blue using a mixed catalyst and product analysis by LC/MS, *Chem. Eng. J.*, 157 (2-3), 373–378.
- [16] Oda, A.M., Ferhod, A.S., and Lafta, A.J., 2014, Modification of the photocatalytic activity of zinc oxide by doping silver, *IJSR*, 3 (11), 2133–2139.
- [17] Oda, A.M., Ali, H.H., Lafta, A.J., Esmael, H.A., Jameel, A.A., Mohammed, A.M., and Mubarak, I.J., 2015, Study self-cleaning of Congo red from cotton fabric loaded by ZnO-Ag, *Int. J. Chem.*, 7 (2), 39–48.
- [18] Oda, A.M., Khuder, H., Hashim, R., Rasheed, A., Hasan, A.A., Hazim, H., and Raheem, Z., 2016, Photocatalytic degradation of safranin O by ZnO-Ag loaded on cotton fabric, *Res. J. Pharm. Biol. Chem. Sci.*, 7 (5), 2915–2924.
- [19] Singh, S., Singh, P.K., and Mahalingam, H., 2014, Novel floating Ag<sup>+</sup>-doped TiO<sub>2</sub>/polystyrene photocatalysts for the treatment of dye wastewater, *Ind. Eng. Chem. Res.*, 53 (42), 16332–16340.
- [20] Zandsalimi, Y., Teymouri, P., Soltani, R.D.C., Rezaee, R., Abdullahi, N., and Safari, M., 2015, Photocatalytic removal of Acid Red 88 dye using zinc oxide nanoparticles fixed on glass plates, *J. Adv. Environ. Health Res.*, 3 (2), 102–110.
- [21] Di Mauro, A., Cantarella, M., Nicotra, G., Pellegrino, G., Gulino, A., Brundo, M.V., Privitera, V., and Impellizzeri, G., 2017, Novel synthesis of ZnO/PMMA nanocomposites for photocatalytic applications, *Sci. Rep.*, 7, 40895.
- [22] Kunarti, E.S., Kartini, I., Syoufian, A., and Widyandari, K.M., 2018, Synthesis and photoactivity of Fe<sub>3</sub>O<sub>4</sub>/TiO<sub>2</sub>-Co as a magnetically separable visible light responsive photocatalyst, *Indones. J. Chem.*, 18 (3), 403–410.
- [23] Chae, D.W., and Kim, B.C., 2005, Characterization on polystyrene/zinc oxide nanocomposites prepared from solution mixing, *Polym. Adv. Technol.*, 16 (11-12), 846–850.
- [24] Kaniappan, K., and Latha, S., 2011, Certain investigations on the formulation and characterization of polystyrene/poly(methyl methacrylate) blends, *Int. J. ChemTech Res.*, 3 (2), 708–717.

- [25] Sangawar, V.S., and Golchha, M.C., 2013, Evolution of the optical properties of polystyrene thin films filled with zinc oxide nanoparticles, *Int. J. Sci. Eng. Res.*, 4 (6), 2700–2705.
- [26] Zhou, X.D., Xiao, X.H., Xu, J.X., Cai, G.X., Ren, F., and Jiang, C.Z., 2011, Mechanism of the enhancement and quenching of ZnO photoluminescence by ZnO-Ag coupling, *Europhys. Lett.*, 93 (5), 57009.
- [27] Aazam E.S., 2014, Visible light photocatalytic degradation of thiophene using Ag-TiO<sub>2</sub>/multi-walled carbon nanotubes nanocomposite, *Ceram. Int.*, 40 (5), 6705–6711.
- [28] Ren, C., Yang, B., Wu, M., Xu, J., Fu, Z., Lv, Y., Guo, T., Zhao, Y., and Zhu, C., 2010, Synthesis of Ag/ZnO nanorods array with enhanced photocatalytic performance, *J. Hazard. Mater.*, 182 (1-3), 123–129.
- [29] Subash, B., Krishnakumar, B., Swaminathan, M., and Shanthi, M., 2013, Highly efficient, solar active, and reusable photocatalyst: Zr-loaded Ag-ZnO for reactive red 120 dye degradation with synergistic effect and dye-sensitized mechanism, *Langmuir*, 29 (3), 939–949.
- [30] Fageria, P., Gangopadhyay, S., and Pande, S., 2014, Synthesis of ZnO/Au and ZnO/Ag nanoparticles and their photocatalytic application using UV and visible light, *RSC Adv.*, 4 (48), 24962–24972.
- [31] Saravanan, R., Khan, M.M., Gupta, V.K., Mosquera, E., Gracia, F., Narayanan, V., and Stephen, A., 2015, ZnO/Ag/Mn<sub>2</sub>O<sub>3</sub> nanocomposite for visible light-induced industrial textile effluent degradation, uric acid and ascorbic acid sensing and antimicrobial activity, *RSC Adv.*, 5 (44), 34645–34651.
- [32] Byrappa, K., Subramani, A.K., Ananda, S., Rai, K.M.L., Dinesh, R., and Yoshimura, M., 2006, Photocatalytic degradation of rhodamine B dye using hydrothermally synthesized ZnO, *Bull. Mater. Sci.*, 29 (5), 433–438.
- [33] Patchaiyappan, A., Saran, S., and Devipriya, S.P., 2016, Recovery and reuse of TiO<sub>2</sub> photocatalyst from aqueous suspension using plant based coagulant-A green approach, *Korean J. Chem. Eng.*, 33 (7), 2107–2113.
- [34] Krishnakumar, B., Subash, B., and Swaminathan, M., 2012, AgBr-ZnO-An efficient nano-photocatalyst for the mineralization of acid black 1 with UV light, *Sep. Purif. Technol.*, 85, 35–44.
- [35] Saravanan, R., Khan, M.M., Gupta, V.K., Mosquera, E., Gracia, F., Narayanan, V., and Stephen, A., 2015, ZnO/Ag/CdO nanocomposite for visible light-induced photocatalytic degradation of industrial textile effluents, *J. Colloid Interface Sci.*, 452, 126–133.